

CONTROL OF SHUNT ACTIVE FILTER BASED ON THE INTERNAL MODEL PRINCIPLE: TUNING PROCEDURE AND EXPERIMENTAL RESULTS

F. Ronchi *, A. Tilli *, L. Marconi *

* CASY - Center for Research on Complex Automated Systems “G. Evangelisti”
DEIS - University of Bologna - Viale Risorgimento n.2, 40136 Bologna, ITALY
Tel. +39 051 20 93024 , Fax. +39 051 20 93073, E-mail: { fronchi, atilli, lmarconi }@deis.unibo.it

Keywords: Active filters, Control system design, Digital control, Discrete-time systems.

Abstract

Shunt active filters are used to compensate for electric current harmonics in the line grid. In this paper the internal model principle is exploited to achieve asymptotic harmonics cancellation. A detailed tuning procedure for this kind of controller is provided, keeping into account the effects of digital implementation. Extensive experimental results show the effectiveness of the proposed approach.

1 Introduction

AC sinusoidal mains are polluted by nonlinear loads generating undesired harmonics in the electric currents. This effect determines additional power losses and the risk of equipment damage or malfunctioning. Hence, some countermeasures have to be taken to reduce this harmonic distortion. Passive filters have been traditionally adopted to compensate for current harmonics. The main drawbacks of these devices are: dependance on the network impedance, impossibility of simple reconfiguration. In the last decades, the fast development of power electronics components and control processors has led to the introduction of the so-called Active Power Filters (APF) [3]. These devices can be more expensive than the passive filters, but they are less network-dependant and can be tuned on different frequencies changing a few software parameters.

A particular kind of APF are the Shunt Active Filters (SAF), whose purpose is to inject into the mains a proper current in order to compensate partially or totally for the harmonic current generated by nonlinear loads [10]. The SAF considered in this paper are based on AC/DC three-phases boost converter topology and they are connected in parallel to the distorting loads as it is shown in Fig.1. Different approaches dealing with this kind of SAF have been presented in literature [3],[4]. The main distinguishing marks are the filter current control algorithm and the load current analysis methods adopted to determine the filter current objective. In [7], [6], [5] different current control solutions have been developed. In [6], the high performances of hysteresis current controllers are exploited. As regards the generation of filter current references, the instantaneous power the-

ory [2], the time-domain correlation techniques [14], the Fast Fourier Transform and some other methods have been used to detect the load current harmonics. In [9] the authors adopted the Internal Model Principle to merge the filter control problem and the the load harmonics detection.

In this paper, the Internal Model Principle is exploited to achieve asymptotic cancellation of current harmonics and a particular solution is adopted to obtain an “easy to tune” controller for the SAF, keeping into account the effects of digital implementation of the proposed solution. The so-called $(d - q)$ reference frame aligned with the mains voltage vector is adopted to distinguish instantaneous active and reactive powers. The exogenous system describing the load model is a bank of oscillators with known frequencies multiples of the line frequency. A particular procedure is developed to assign the closed-loop dynamics, it is based on a suitable design of the zero dynamics of the system. In the discrete-time case particular attention is paid to the effect of the sampling time choice and the computation delay.

The regulation of the SAF DC-link voltage is considered and some preliminary results concerning the coordination between voltage and current control are given. Extensive experimental tests show the effectiveness of the proposed solution.

The paper is organized as follows. In Section 2 the model of the adopted SAF is reported and the control objectives are defined. Some attention is paid to the control objectives feasibility recalling the results of [12]. In Section 3 the proposed controller based on Internal Model Principle is presented and deeply discussed. In Section 4 the proposed controller is suitably tuned to cope with discrete time implementation. In Section 5 some experimental results are provided to enlighten the controller performances.

2 Mathematical model and problem statement

The scheme of the active filter considered in this article is presented in Fig.1. It is a three-phase AC/DC boost converter, where the capacitor is the main energy storage element and the inductors are used for the control of the filter currents by means of the converter voltages. In Fig.1: v_{ma}, v_{mb}, v_{mc} are the mains voltages, i_{ma}, i_{mb}, i_{mc} are the mains currents, i_{la}, i_{lb}, i_{lc} are the load currents, i_a, i_b, i_c are the filter currents, v is the capacitor voltage, L is the value of the inductances,

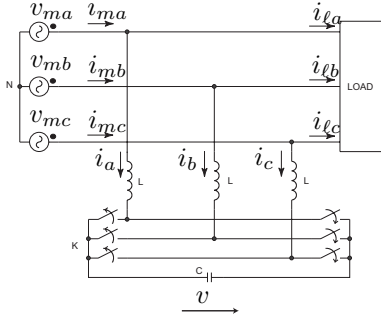


Figure 1: Shunt active filter scheme

C is the value of the DC-bus capacitor. The switches of the three-legs-bridge (usually indicated as “inverter”) are usually realized by IGBTs and free-wheeling diodes

2.1 Mathematical model

The filter model can be described in the $\alpha - \beta$ reference frame as follows [13], [8]

$$\begin{aligned} \frac{d \mathbf{i}_{\alpha\beta}}{dt} &= -\frac{R}{L} \mathbf{I}_2 \mathbf{i}_{\alpha\beta}(t) - \frac{v(t)}{L} \mathbf{u}_{\alpha\beta}(t) + \frac{1}{L} \begin{bmatrix} v_{m\alpha}(t) \\ v_{m\beta}(t) \end{bmatrix} \\ \frac{dv}{dt} &= \frac{3}{2C} \mathbf{u}_{\alpha\beta}^T(t) \mathbf{i}_{\alpha\beta}(t) \end{aligned} \quad (1)$$

with $\mathbf{i}_{\alpha\beta}(t) = {}^{\alpha\beta} T_{abc} \mathbf{i}_{abc}(t)$, $\mathbf{u}_{\alpha\beta}(t) = {}^{\alpha\beta} T_{abc} \mathbf{u}_{abc}(t)$ and

$$\begin{bmatrix} v_{m\alpha} \\ v_{m\beta} \end{bmatrix} = {}^{\alpha\beta} T_{abc} \begin{bmatrix} v_{ma} \\ v_{mb} \\ v_{mc} \end{bmatrix} (t), \quad {}^{\alpha\beta} T_{abc} = \frac{2}{3} \begin{bmatrix} 1 & -\frac{1}{2} & -\frac{1}{2} \\ 0 & \frac{\sqrt{3}}{2} & -\frac{\sqrt{3}}{2} \end{bmatrix}$$

In particular, the control input $\mathbf{u}_{abc}(t)$ is assumed continuous and it has to belong to the hexagon of Fig. 2 in order to be implemented via PWM techniques.

According to the hypothesis of three-phase balanced sinusoidal line, the ideal mains voltages can be expressed as follows

$$\begin{bmatrix} v_{m\alpha}(t) \\ v_{m\beta}(t) \end{bmatrix}^T = V_m \begin{bmatrix} \cos(\omega_m t) \\ \sin(\omega_m t) \end{bmatrix}^T$$

with $\omega_m = 2\pi f_m$ known constant ($f_m \in \{50, 60\}$ Hz according to the country).

It is assumed that the inductance and the capacitance values L , C are known, whereas the parasitic resistance value R is unknown but constant.

Load currents i_{la} , i_{lb} , i_{lc} , filter currents i_a , i_b , i_c and the DC-link voltage v are measured.

The main voltage angle ($\omega_m t$) is reconstructed via PLL techniques.

2.2 Problem statement

The control objective of the proposed active filter is to compensate for the harmonic distortion of the load current, keeping the

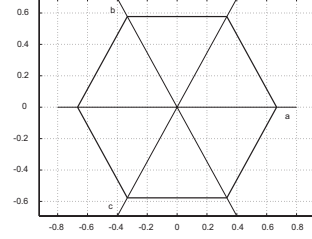


Figure 2: Control input hexagon

DC-link voltage $v(t)$ in the given admissible range. A mathematical formulation of this goal is obtained in the following.

According to the usual behavior of nonlinear loads, the load current $[i_{l\alpha}, i_{l\beta}]^T = {}^{\alpha\beta} T_{abc} [i_{la}(t), i_{lb}(t), i_{lc}(t)]^T$, can be assumed periodic with frequency f_m and it can be expressed as

$$\begin{aligned} i_{l\sigma}(t) &= I_{l\sigma 0} + I_{l\sigma 1} \cos(\omega_m t + \varphi_{l\sigma 1}) + \\ &+ \sum_{n=2}^{\infty} I_{l\sigma n} \cos(n\omega_m t + \varphi_{l\sigma n}), \quad \sigma = \alpha, \beta \end{aligned}$$

The instantaneous real power absorbed by the load can be calculated as

$$p_\ell(t) = \frac{3}{2} \begin{bmatrix} v_{m\alpha} \\ v_{m\beta} \end{bmatrix}^T \begin{bmatrix} i_{l\alpha} \\ i_{l\beta} \end{bmatrix} = P_{\ell 0} + \sum_{n=1}^{\infty} P_{\ell n} \cos(n\omega_m t + \psi_n)$$

where the constant term $P_{\ell 0}$

$$P_{\ell 0} = \frac{3}{2} (V_m I_{l\alpha 1} \cos \varphi_{l\alpha 1} + V_m I_{l\beta 1} \cos \varphi_{l\beta 1})$$

is the only component really useful in delivering energy to the load. The remaining part has a null balance over each line period and it should be removed from the instantaneous power required to the line grid in order to reduce line current level [11]. The instantaneous imaginary power [1] absorbed by the load can be calculated as

$$q_\ell(t) = \frac{3}{2} \begin{bmatrix} -v_{m\beta} \\ v_{m\alpha} \end{bmatrix}^T \begin{bmatrix} i_{l\alpha} \\ i_{l\beta} \end{bmatrix} = Q_{\ell 0} + \sum_{n=1}^{\infty} Q_{\ell n} \cos(n\omega_m t + \theta_n)$$

The same level of real power p_ℓ correspond to different values of current. A complete cancellation of load imaginary power should be achieved to minimize the current required to the line grid.

Owing to limited elaboration time and physical constraints of the filter, only some of the load harmonics can be compensated for. Hence, the load that is considered for the compensation is constituted by a number N of harmonics.

The main control objective of the proposed SAF can be formulated as follows.

O₁ The instantaneous real power absorbed by the SAF, $p(t) = \frac{3}{2} \begin{bmatrix} v_{m\alpha}(t) & v_{m\beta}(t) \end{bmatrix} \mathbf{i}_{\alpha\beta}(t)$ has to asymptotically compensate for the oscillating component of the load real

power, i.e.

$$\lim_{t \rightarrow \infty} (p(t) + p_\ell(t)) = P_{\ell 0} + P_{f 0}$$

where $P_{f 0}$ is a constant term which compensate for the power losses in the SAF.

The instantaneous imaginary power absorbed by the SAF $q(t) = \frac{3}{2} [-v_{m\beta}(t) \ v_{m\alpha}(t)] \mathbf{i}_{\alpha\beta}(t)$ has to asymptotically compensate for the load imaginary power, i.e.

$$\lim_{t \rightarrow \infty} (q(t) + q_\ell(t)) = 0$$

The above control objective must be achieved keeping the DC-link voltage $v(t)$ inside an admissible range $[V_{min}, V_{max}]$. As deeply discussed in [12], the lower bound V_{min} is defined according to a ‘‘current controllability constraint’’. In plain words, the DC-link voltage has to be large enough to compensate for the line voltage and to steer the current delivered by the filter. Differently, the upper bound V_{max} depends on the maximum ratings of the adopted capacitor. Hence, a second control objective has to be defined as follows.

O₂ The DC-link voltage $v(t)$ must be kept within the admissible range $[V_{min}, V_{max}]$, $\forall t > t_0$. It is assumed that at time $t = t_0$ the harmonic compensation algorithm is started and $v(t_0) \in [V_{min}, V_{max}]$. This hypothesis about $v(t_0)$ is coherent with actual behavior of SAF [11] because the first operation that is performed when the SAF is ‘‘turned on’’ is to increase the DC-link voltage to a suitable value $\bar{V} \in [V_{min}, V_{max}]$. The SAF control algorithm is started only after this operation.

Following the procedure reported in [12] it can be shown that **O₁** and **O₂** are not in contrast if and only if a suitable design of the capacitor and inductor values is carried-out, given a worst-case for the load power to compensate for. As already enlightened, in the control design the load and filter currents, the mains voltages angles are assumed known from measurements.

3 Controller design

As first step, the model (1) state variables are translated into the $d - q$ synchronous reference frame as follows

$$\mathbf{x} = \begin{bmatrix} x_d \\ x_q \end{bmatrix} = {}^{dq} T_{\alpha\beta}(t) \mathbf{i}_{\alpha\beta}, \quad \mathbf{u} = \begin{bmatrix} u_d \\ u_q \end{bmatrix} = {}^{dq} T_{\alpha\beta}(t) \mathbf{u}_{\alpha\beta},$$

$${}^{dq} T_{\alpha\beta}(t) = \begin{bmatrix} \cos(\omega_m t) & \sin(\omega_m t) \\ -\sin(\omega_m t) & \cos(\omega_m t) \end{bmatrix}$$

The SAF model becomes

$$\dot{\mathbf{x}}(t) = \left(-\frac{R}{L} I_2 + \omega_m \begin{bmatrix} 0 & 1 \\ -1 & 0 \end{bmatrix} \right) \mathbf{x}(t) - \frac{v(t)}{L} \mathbf{u}(t) + \begin{bmatrix} \frac{V_m}{L} \\ 0 \end{bmatrix}$$

$$\dot{v}(t) = \frac{3}{2C} \mathbf{u}^T(t) \mathbf{x}(t) \quad (2)$$

The current reference $\mathbf{x}^* = [x_d^*, x_q^*]^T$ is designed to mainly offset the undesired load components, introducing a stabilizing action for the $v(t)$ dynamics when the DC-link voltage approaches unsafe values. Under this perspective, the variable

$x_d(t)$ is seen as a virtual control input for the voltage dynamics, as it is explained in the next subsection.

The SAF controller is then composed by two parts: a DC-link voltage regulator which guarantees objective **O₂** acting on x_d^* and a current controller which purpose is to achieve objective **O₁** and to track the current command from the voltage regulator.

3.1 Current controller

Defining the tracking error $\tilde{\mathbf{x}} = \mathbf{x} - \mathbf{x}^*$ and assuming the main voltage amplitude V_m can be written as the sum of the nominal value \bar{V}_m and a constant unknown value \tilde{V}_m , the model (2) can be rewritten as

$$\dot{\tilde{\mathbf{x}}}(t) = \frac{1}{L} \left\{ \left(-RI_2 + \begin{bmatrix} 0 & \omega_m L \\ -\omega_m L & 0 \end{bmatrix} \right) (\tilde{\mathbf{x}}(t) + \mathbf{x}^*(t)) \right. \\ \left. -v(t) \mathbf{u}(t) + \begin{bmatrix} \bar{V}_m \\ 0 \end{bmatrix} + \begin{bmatrix} \tilde{V}_m \\ 0 \end{bmatrix} - L\dot{\mathbf{x}}^* \right\}$$

$$\dot{v}(t) = \frac{3}{2C} \mathbf{u}^T(t) (\tilde{\mathbf{x}}(t) + \mathbf{x}^*(t)) \quad (3)$$

The following preliminary control action is performed to linearize and decouple the current dynamics

$$\mathbf{u}(t) = \frac{1}{v(t)} \left(\begin{bmatrix} \bar{V}_m \\ 0 \end{bmatrix} + \begin{bmatrix} 0 & \omega_m L \\ -\omega_m L & 0 \end{bmatrix} \mathbf{x}(t) - \mathbf{u}_1(t) \right)$$

Implementing this control and defining

$$\mathbf{d}(t) = \begin{bmatrix} d_d(t) \\ d_q(t) \end{bmatrix} = \begin{bmatrix} \tilde{V}_m \\ 0 \end{bmatrix} - R I_2 \mathbf{x}^*(t) - L\dot{\mathbf{x}}^*$$

the two current dynamics of (3) can be divided into two equations having the same following mathematical form

$$\dot{\tilde{x}}(t) = \frac{1}{L} \{ -R\tilde{x}(t) + u_1(t) + d(t) \} \quad (4)$$

where the subscripts d or q are omitted. This one-dimensional model is considered in the following.

The signal $d(t)$ can be decomposed into the sum of two terms $d_n(t)$ and $d_{im}(t)$. The former is fully unknown, whereas the latter is sum of a constant and sinusoids having known frequencies (they correspond to the load harmonics that have to be compensated for). Hence, the signal $d_{im}(t)$ can be seen as the output of the following linear system.

$$\dot{\mathbf{w}}(t) = \Omega \mathbf{w}(t), \quad d_{im}(t) = \Gamma \mathbf{w}(t) \quad (5)$$

with $\Gamma = \begin{bmatrix} 1 & 1 & 0 & \dots & 1 & 0 \end{bmatrix}$ and $\Omega = \text{blockdiag} \{ S_0, S_1, \dots, S_{N+1} \}$,

$$S_0 = 0, \quad S_k = k\omega_m \begin{bmatrix} 0 & 1 \\ -1 & 0 \end{bmatrix}, \quad k = 1, \dots, N+1$$

The following linear controller is considered

$$\dot{\hat{\mathbf{w}}} = \Omega \hat{\mathbf{w}} + \Theta k_0 \nu, \quad u_1 = -\Gamma \hat{\mathbf{w}} + k_0 \nu \quad (6)$$

with $\nu = -\tilde{x}$. Defining the estimation error $\tilde{\mathbf{w}} = \hat{\mathbf{w}} - \mathbf{w}$, the sum of the signals $u_1(t)$ and $d(t)$ can be seen as the output of the following LTI system

$$\dot{\tilde{\mathbf{w}}} = \Omega \tilde{\mathbf{w}} + \Theta k_0 \nu, \quad u_1 + d_{im} = -\Gamma \tilde{\mathbf{w}} + k_0 \nu$$

The open loop system can be described as follows

$$\begin{bmatrix} \dot{\tilde{x}} \\ \dot{\tilde{w}} \end{bmatrix} = \begin{bmatrix} -\frac{R}{L} & -\frac{1}{L}\Gamma \\ 0 & \Omega \end{bmatrix} \begin{bmatrix} \tilde{x} \\ \tilde{w} \end{bmatrix} + \begin{bmatrix} \frac{k_0}{L} \\ \Theta k_0 \end{bmatrix} \nu + \begin{bmatrix} \frac{d_n(t)}{L} \\ 0 \end{bmatrix} \quad (7)$$

The poles of this open loop LTI system are in $-\frac{R}{L}$, 0 , $\pm jk \omega_m$, $k = 1, \dots, N+1$. Assuming $d_n(t) = 0$, the zero dynamic of the open loop system with respect to the output \tilde{x} can be calculated imposing $(u_1(t) + d_{im}(t)) = 0$. It follows

$$\dot{\tilde{w}}_0 = (\Omega + \Theta\Gamma) \tilde{w}_0$$

Being (Ω, Γ) observable, the zeros of system (7) can be arbitrarily placed by means of Θ . In particular, they can be chosen with negative real part and then it is easy to show that there exists a \bar{k}_0 such that $\forall k_0 > \bar{k}_0$ the resulting closed loop system is globally asymptotically stable.

Then, the resulting control law \mathbf{u} can be written as

$$\begin{aligned} \begin{bmatrix} \dot{\hat{\mathbf{w}}_d} \\ \dot{\hat{\mathbf{w}}_q} \end{bmatrix} &= \begin{bmatrix} \Omega & 0 \\ 0 & \Omega \end{bmatrix} \begin{bmatrix} \hat{\mathbf{w}}_d \\ \hat{\mathbf{w}}_q \end{bmatrix} - \begin{bmatrix} \Theta k_0 & 0 \\ 0 & \Theta k_0 \end{bmatrix} \begin{bmatrix} \tilde{x}_d \\ \tilde{x}_q \end{bmatrix} \\ \mathbf{u}(t) &= \frac{1}{v(t)} \left(\begin{bmatrix} \bar{V}_m \\ 0 \end{bmatrix} + \omega_m L \begin{bmatrix} 0 & 1 \\ -1 & 0 \end{bmatrix} \mathbf{x}(t) + \begin{bmatrix} \Gamma & 0 \\ 0 & \Gamma \end{bmatrix} \begin{bmatrix} \hat{\mathbf{w}}_d \\ \hat{\mathbf{w}}_q \end{bmatrix} + k_0 I_2 \begin{bmatrix} \tilde{x}_d \\ \tilde{x}_q \end{bmatrix} \right) \quad (8) \end{aligned}$$

and the current closed loop system becomes

$$\begin{bmatrix} \dot{\tilde{x}}_d \\ \dot{\tilde{w}}_d \\ \dot{\tilde{x}}_q \\ \dot{\tilde{w}}_q \end{bmatrix} = \begin{bmatrix} -\frac{R+k_0}{L} & -\frac{1}{L}\Gamma & 0 & 0 \\ -\Theta k_0 & \Omega & 0 & 0 \\ 0 & 0 & -\frac{R+k_0}{L} & -\frac{1}{L}\Gamma \\ 0 & 0 & -\Theta k_0 & \Omega \end{bmatrix} \begin{bmatrix} \tilde{x}_d \\ \tilde{w}_d \\ \tilde{x}_q \\ \tilde{w}_q \end{bmatrix} + \begin{bmatrix} \frac{d_{nd}(t)}{L} \\ 0 \\ \frac{d_{nq}(t)}{L} \\ 0 \end{bmatrix} \quad (9)$$

3.2 Voltage controller

The adopted control strategy is to introduce a stabilizing action for the $v(t)$ dynamics when the DC-link voltage approaches unsafe values. Under this perspective, the variable $x_d(t)$ is seen as a virtual control input for the voltage dynamics. Hence the current reference can be decomposed as follows

$$\mathbf{x}^*(t) = \mathbf{x}_\ell^*(t) + \mathbf{x}_{\ell n}^* + [x_v^* \ 0]^T$$

where \mathbf{x}_ℓ^* is made of the load harmonics to compensate for, $\mathbf{x}_{\ell n}^*$ is composed by the remaining part of the load harmonics, x_v^* is the voltage controller output.

Defining $e = v^2(t) - \bar{V}^2$ with $\bar{V}^2 = (V_{min}^2 + V_{max}^2)/2$, the voltage controller output is calculated as the output of the following saturated function

$$x_v^*(e) = -k_v \begin{cases} 0 & \text{if } |e| \leq \ell_m \\ e - \ell_m \operatorname{sign}(e) & \text{if } \ell_m < |e| < \ell_M \\ (\ell_M - \ell_m) \operatorname{sign}(e) & \text{if } |e| \leq \ell_M \end{cases}$$

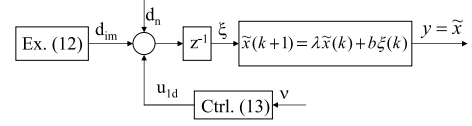


Figure 3: Discrete time open loop system scheme

with $k_v > 0$ and ℓ_m , ℓ_M two design parameters such that $\ell_m < \ell_M \leq (V_{max}^2 - V_{min}^2)/2$. The voltage dynamic can be described as

$$\begin{aligned} \dot{e} &= \frac{3}{C} \left(\begin{bmatrix} \bar{V}_m \\ 0 \end{bmatrix} + \begin{bmatrix} d_{imd}(t) \\ d_{imq}(t) \end{bmatrix} + \begin{bmatrix} \Gamma & 0 \\ 0 & \Gamma \end{bmatrix} \begin{bmatrix} \tilde{w}_d(t) \\ \tilde{w}_q(t) \end{bmatrix} + \right. \\ &\quad \left. + k_0 \begin{bmatrix} \tilde{x}_d(t) \\ \tilde{x}_q(t) \end{bmatrix} \right)^T \left(\begin{bmatrix} \tilde{x}_d(t) \\ \tilde{x}_q(t) \end{bmatrix} + \mathbf{x}_\ell^* + \mathbf{x}_{\ell n}^* + \begin{bmatrix} x_v^* \\ 0 \end{bmatrix} \right) \quad (10) \end{aligned}$$

Assuming a two time scale behavior for the system (this is supported by experimental results), it can be assumed that \tilde{x} and \tilde{w} in (10) are negligible, while x_v^* is almost constant in the current dynamics. Hence, the x_v^* term produces the power P_{f0} of the objective O_1 . If C is sufficiently high and k_0 is properly designed, then the two time scales behavior holds and the proposed controller works. A more precise and complete stability analysis will be addressed in future works on this subject.

Remark: The not-compensated harmonics d_{nd} and d_{nq} are bounded perturbations for the stable dynamics (9). Their effects can be avoided if a suitable model based prefiltering of the load current is performed according to [13].

4 Discrete time controller tuning

In order to implement the controller (8) on a DSP-based architecture, a discrete time tuning of the control parameters is performed. The main additional trouble to cope with is the delay of a sampling time T_s due to the elaboration time. Assuming that the effects of this delay on the feedback linearizing part of (8) are negligible, only the linear part of the controller is tuned.

For the sake of brevity, in this section it is assumed that $d_n = 0$ and then $d_{im} = d$. The (4) and (5) are discretized according to the “zero-order-holder” method, obtaining

$$\tilde{x}(k+1) = \lambda \tilde{x}(k) + b(u_1(k) + d(k)) \quad (11)$$

$$\mathbf{w}(k+1) = \Omega_z \mathbf{w}(k) \quad (12)$$

$$d(k) = \Gamma \mathbf{w}(k)$$

with $\lambda = e^{-\frac{R}{L}T_s}$, $b = \frac{1}{R}(1 - e^{-\frac{R}{L}T_s})$ and $\Omega_z = \text{blockdiag}(S_{z0}, S_{z1}, \dots, S_{zn})$,

$$S_{z0}=1, S_{zk} = \begin{bmatrix} \cos(k\omega_m T_s) & \sin(k\omega_m T_s) \\ -\sin(k\omega_m T_s) & \cos(k\omega_m T_s) \end{bmatrix}, k=1, \dots, N+1$$

The delay of one sampling time T_s can be managed adding one state v to the (11)

$$\begin{bmatrix} v(k+1) \\ \tilde{x}(k+1) \end{bmatrix} = \begin{bmatrix} 0 & 0 \\ 1 & \lambda_1 \end{bmatrix} \begin{bmatrix} v(k) \\ \tilde{x}(k) \end{bmatrix} + \begin{bmatrix} b \\ 0 \end{bmatrix} (u_1(k) + d(k))$$

The controller (6) can be implemented as follows

$$\begin{aligned}\hat{\mathbf{w}}(k+1) &= \Omega_z \hat{\mathbf{w}}(k) + \Theta_z k_0 \nu(k) \\ u_1(k) &= -\Gamma \hat{\mathbf{w}}(k) + k_0 \nu(k)\end{aligned}\quad (13)$$

with $\nu(k) = -\tilde{x}(k)$. Defining $\tilde{\mathbf{w}}(k) = \hat{\mathbf{w}}(k) - \mathbf{w}(k)$, the controller becomes

$$\begin{aligned}\tilde{\mathbf{w}}(k+1) &= \Omega_z \tilde{\mathbf{w}}(k) + \Theta_z k_0 \nu(k) \\ u_1(k) &= -\Gamma \tilde{\mathbf{w}}(k) - d(k) + k_0 \nu(k)\end{aligned}$$

The open loop system scheme is shown in Fig. 3.

Defining

$$F = \begin{bmatrix} \lambda_1 & 1 & 0 \\ 0 & 0 & -b\Gamma \\ 0 & 0 & \Omega_z \end{bmatrix}, \quad g = \begin{bmatrix} 0 \\ b k_0 \\ \Theta_z k_0 \end{bmatrix}, \quad h = \begin{bmatrix} 1 \\ 0 \\ 0 \end{bmatrix}$$

the open-loop system becomes

$$\begin{bmatrix} \tilde{x}_d(k+1) \\ v(k+1) \\ \tilde{\mathbf{w}}_d(k+1) \end{bmatrix} = F \begin{bmatrix} \tilde{x}_d(k) \\ v(k) \\ \tilde{\mathbf{w}}_d(k) \end{bmatrix} + g\nu(k), \quad y(k) = h^T \begin{bmatrix} \tilde{x}_d(k) \\ v(k) \\ \tilde{\mathbf{w}}_d(k) \end{bmatrix}\quad (14)$$

The poles of this discrete-time system are $0, \lambda_1, 1, e^{\pm jk\omega_m T_s}, k = 1, \dots, N+1$. Its relative degree is two. The zero dynamic of the open loop system can be calculated imposing $u_1 + d_{im} = 0$. It follows

$$(\tilde{w}(k+1))_0 = (\Omega + \Theta_z \Gamma) (\tilde{w}(k))_0$$

Being (Ω_z, Γ) observable, the zeros of system (14) can be arbitrarily placed by means of Θ .

Assuming the following parameters for the filter: $\overline{V}_m = 220\sqrt{2} V$, $\omega_m = 2\pi 50 \text{ rad/s}$, $R = 0.12 \Omega$, $L = 3 \text{ mH}$, $C = 4400 \mu\text{F}$ and the sampling time $T_s = 14.336 \text{ ms}$, if the load harmonics to compensate for are $\omega_6 = 6\omega_m$ and $\omega_{12} = 12\omega_m$, then the following parameters are chosen for the controller (13).

$$\Theta_z = 10^3 \begin{bmatrix} -4.472 & 0.717 & 27.574 & -1.964 & 64.278 \end{bmatrix}^T$$

$\Gamma = [1 \ 1 \ 0 \ 1 \ 0]$ and $k_0 = 10$. The above Θ_z places the zeros of the loop function within the unity circle and very near to the poles, as shown in the root locus of Fig. 4. In this way the resulting closed loop system is globally asymptotically stable and the rejection of the disturb d is characterized by the transfer function which Bode diagram is shown in Fig. 5.

The choice of the zeros position is critical with respect to the adopted sampling time. The root locus of Fig. 4 mainly reproduces the behavior of the continuous time version, except for the vertical divergent branches due to the unit delay. If zeros are placed far away from poles towards the real axis, then the root locus has a completely different shape which can lead to instability even for small values of k_0 . Moreover, even if instability does not arise, the resonance peaks become higher in the Bode diagram of the closed loop system. The maximum distance between the poles and zeros which does not produce the above effects is proportional to the sampling time value.

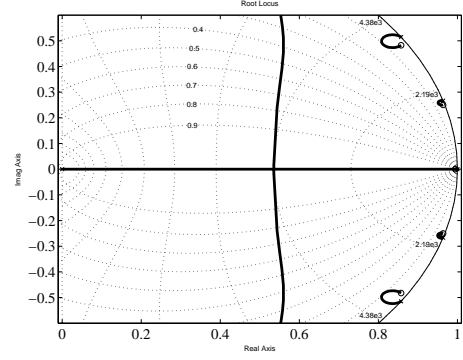


Figure 4: Root Locus w.r.t the current reference.

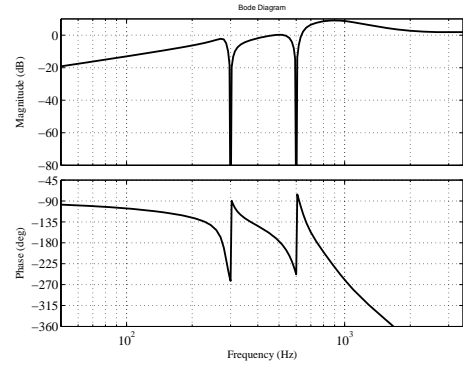


Figure 5: Sensitivity function w.r.t the current reference.

5 Experimental results

The Shunt Active Filter adopted for experimental tests is characterized by the following parameters: $L = 3 \text{ mH}$, $C = 4400 \mu\text{F}$, $V_{min} = 700 V$, $V_{max} = 900 V$, $I_{max} = 100 A$, $\ell_{max} = 160000$, $\ell_{min} = 16000$, $k_v = 0.00016$ and the same Θ_z, k_0 of the previous section. The load currents, i_{la}, i_{lb} , and the filter currents, i_a, i_b have been measured by means of closed-loop Hall sensors. The line voltages have been detected using Voltage Transformers, while the DC-link voltage has been measured with a voltage Hall sensor. A DSP board based on the TMS320C32 has been used to implement the proposed control strategy. The adopted sampling frequency $f_s = 1/T_s$ is equal to 7 kHz , as the PWM carrier frequency.

A balanced nonlinear load is the benchmark for the proposed solution. It is the sum of an electric motor with no load and of a lamp bank fed by means of a diode rectifier. Its phase-a current is shown in fig. 6(a), together with the phases a of main voltages and currents. The Fast Fourier Transform of the d-q components of load and mains currents is shown in figs. 6(b) and 6(c). It can be noted that the 6th and 12th load current harmonics are fully eliminated, whereas the 18th is little amplified. The reason of this is straightforward looking at the Bode diagram of Fig. 5 Hence, the tuning of the current controller is crucial for not increasing the non-compensated harmonics. Anyway, this effect can be totally avoided with a suitable model

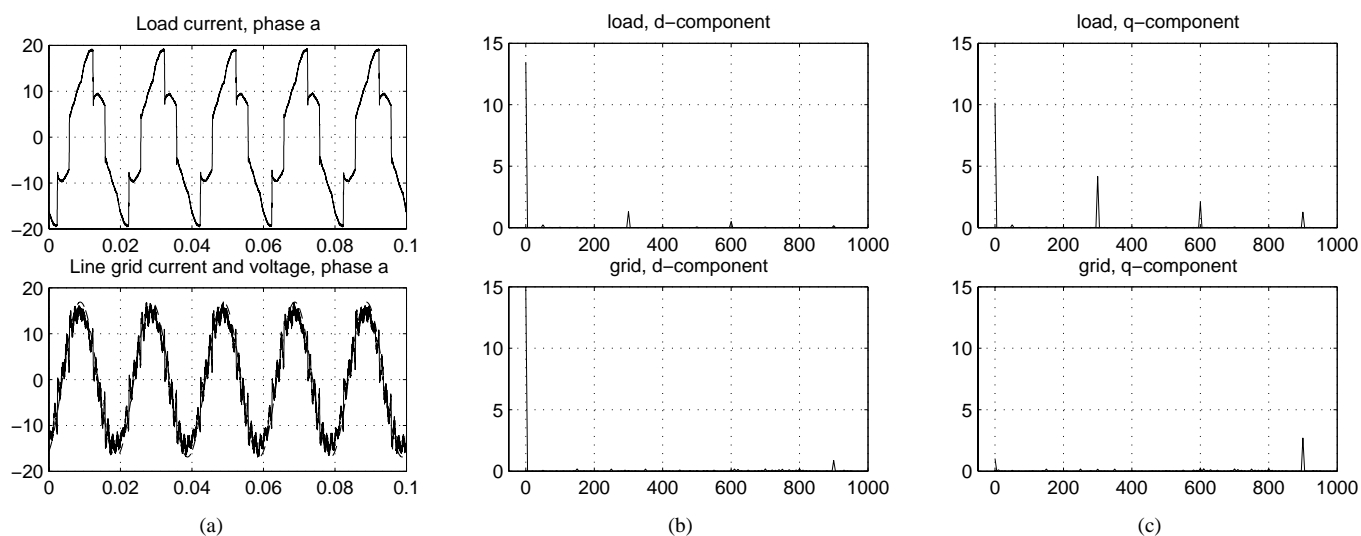


Figure 6: a) Phase a, load current (A), main current (A) and voltage (dashed and scaled). b-c) FFTs of the d and q components of load and main currents

based prefiltering [13].

6 Conclusions

An internal model based controller for shunt active filters has been proposed. This solution provides asymptotic cancellation of the current harmonics explicitly considered in the controller internal model. A tuning procedure is developed in order to deal with the digital implementation of the proposed algorithm. Experimental results enlighten the promising performances of the presented solution.

In future works particular attention will be devoted to some issues not completely addressed in this paper, such as a deeper coordination between the current and voltage controllers, the evaluation/compensation of the time delay effects for the linearizing control law and a merge between the partial and selective compensation approach proposed in [13] and the control technique proposed in this paper.

References

- [1] H. Akagi, Y. Kanagawa, A. Nabae "Instantaneous reactive power compensator comprising switching devices without energy storage components", *IEEE Trans. on Ind. Applic.* volume IA-20, pp. , (May/June. 1984).
- [2] H. Akagi, A. Nabae. "Control strategy of active power filters using multiple voltage source PWM converters", *IEEE Trans. Ind. Applicat.*, volume IA-22, pp. 460–465, (May/June 1986).
- [3] H. Akagi. "New trends in active filters for power conditioning", *IEEE Trans. Ind. Applicat.*, volume 32, pp. 1312–1332, (Nov./Dec. 1996).
- [4] Bhim Singh, Kamal Al-Haddad. "A review of active filters for power quality improvement", *IEEE Trans. Ind. Elect.*, volume 46, no.5, pp. 960–971, (Oct. 1999).
- [5] S. Buso, L. Malesani, P. Mattavelli, R. Veronese "Design and fully digital control of parallel active filters for thyristor rectifiers to comply with IEC-100-3-2", *IEEE Trans. Ind. Application.* volume 34, pp. 508–517, (May/June 1998).
- [6] A. Chandra, B. Singh, B. N. Singh, K. Al-Haddad "An improved control algorithm of shunt active filter for voltage regulation, harmonic elimination, power-factor correction, and balancing of nonlinear loads", *IEEE Trans. Power Electron.* volume 15, pp. 495–507, (May 2000).
- [7] G. Escobar Valderrama, P. Mattavelli, A. M. Stanković "Reactive Power and Unbalance Compensation Using STATCOM with Dissipativity-Based Control", *IEEE Trans. Control Systems Technology* volume 9, pp. 718–727, (September 2001).
- [8] P. C. Krause, O. Wasynczuk, S. D. Sudhoff. *Analysis of Electric Machinery*, IEEE Press, Piscataway, NY (USA), 1995.
- [9] L. Marconi, F. Ronchi, A. Tilli "Robust control of shunt active filters based on the internal model principle", *submitted to ACC 2003*, Denver, Colorado USA, June 2003.
- [10] P. Mattavelli. "A closed-loop selective harmonic compensation for active filters", *IEEE Trans. Ind. Applicat.*, volume 37, pp. 81–89, (January/February 2001).
- [11] N. Mohan, T. M. Undeland, W. P. Robbins. *Power Electronics. Converters, Applications and Design*, 2nd Ed., John Wiley & sons inc., New York, NY (USA), 1989.
- [12] F. Ronchi, A. Tilli "Design methodology for shunt active filters", *Proc. 10th EPE-PEMC 2002*, Cavtat & Dubrovnik, Croatia, September 2002.
- [13] A. Tilli, F. Ronchi, A. Tonielli "Shunt active filters: selective compensation of current harmonics via state observer", *Proc. IECON 2002*, Sevilla, Spain, November 2002.
- [14] G. L. Van Harmelen, J. H. R. Enslin "Real-time dynamic control of dynamic power filters in supplies with high contamination", *IEEE Trans. Power Electron.* volume 8, pp. 301–308, (Oct. 1993).